IL NUOVO CIMENTO Vol. 26 C, N. 2 Marzo-Aprile 2003

Tropospheric and stratospheric aspects of the North Atlantic Oscillation: An eddy perspective

P. M. Ruti([1])(*) and A. Sutera([2])

([1]) *ENEA-C.R. Casaccia, Gruppo di Dinamica Atmosferica e Oceanica V. Anguillarese 301, 00060 S. Maria di Galeria (Roma), Italy*
([2]) *Dipartimento di Fisica, Università di Roma "La Sapienza" - Roma, Italy*

(ricevuto l'1 Marzo 2002; revisionato il 15 Marzo 2003; approvato l'11 Aprile 2003)

Summary. — Recent studies have described the leading patterns of variability of the Northern Hemisphere extratropical circulation as an annular structure. The associated sea-level winter feature resembles the North Atlantic Oscillation pattern; however, it has been noticed that its centers of action, covering most of the Arctic, have a more zonally symmetric structure. This mode has been referred as the Arctic Oscillation (AO). By considering the vertical structure of the AO, some authors have suggested that a stratosphere-troposphere interaction mechanism may be the source of the interannual variability associated with the AO and, therefore, it could have some relevances also for the NAO. Thus, the NAO and the AO may be considered as different facets of the same phenomenon. In the present paper we analyze the interannual variability of 52 Northern hemisphere winters in the NCEP reanalysis. The study rests on a principal component analysis and singular value decomposition of the sea level pressure, the geopotential heights at 500 hPa and 50 hPa and the zonal wind at 200 hPa. Moreover, following Rossby earlier works, we compute the principal components also for the eddy fields. The analysis performed suggests that the eddy patterns of variability allow a better identification of the modes connected to the NAO in the middle troposphere and in the lower stratosphere. Two distinct stratospheric wave patterns are found to be related to NAO and PNA modes. The covariance analysis suggests a dynamical link with the Atlantic jet exit for the former mode, and a connection with the Atlantic jet entrance for the latter mode. In view of the NAO-AO debate, the results here presented seem to confirm that the NAO and PNA mechanisms contribute separately to the atmospheric eddies variability in the troposphere and in the lower stratosphere.

PACS 92.60.Bh – General circulation.
PACS 92.70.Cp – Atmosphere.
PACS 92.70.Gt – Climate dynamics.
PACS 02.50.Sk – Multivariate analysis.

(*) E-mail: paolo.ruti@casaccia.enea.it

1. – Introduction

An important issue in climate research concerns the nature of the observed interannual variability of the atmospheric flow on a planetary scale. In the last twenty years, starting from the pioneering work of ref. [1], few teleconnection patterns have been identified as the carriers of the interannual atmospheric variability.

In the Northern Hemisphere, a well-documented spatial pattern of extratropical interannual variability is the North Atlantic Oscillation (NAO) [2-4]. The NAO has been mainly identified as a feature of the surface fields fluctuations (sea level pressure and surface temperature), and its definition is often related to the standardized anomaly sea level pressure difference between two precise locations in the Atlantic sector [3].

It is an open question whether the NAO is a phenomenon limited to the Atlantic sector or it is embedded in a larger planetary scale circulation. In this framework, ref. [5] has recently suggested that the NAO pattern can be interpreted as a facet of a global zonally symmetric mode (annular). This mode of variability has been introduced by ref. [6] and has become to be known as the Artic Oscillation (AO). The Artic Oscillation is defined as the leading Empirical Orthogonal Function (EOF) of the wintertime (November-April) mean of the sea level pressure anomaly field. The AO has been interpreted as the surface signature of modulations in the strength of the polar vortex. Moreover, it has been found that the AO variability may have been mirrored by the 50 hPa height variability over the past 30 years; thus the AO may be assumed as a deep vertically coherent mode of variability. Reference [7], describing the Northern (NH) and Southern (SH) hemispheric annular modes, pointed out that the NH mode is often connected with the NH stratospheric circulation during a midwinter season (3-4 months), while the SH mode seems to be linked to the stratosphere circulation in a shorter time window (6-8 weeks).

In ref. [8] a possible long-term trend in few atmospheric fields is showed. The trends in the surface air temperature, precipitation, total column ozone, tropopause pressure and zonal-mean circulation are consistent with the trend in the AO.

This annular perspective has been discussed and criticized in two recent papers [9,10]. In particular in [10] it is concluded that the NAO paradigm may be more physically relevant in the Northern Hemisphere variability compared to the AO perspective.

Several authors (see [11-13], among others) have pointed out a strong connection between tropospheric and stratospheric fields. In particular, in [14] the EOFs of geopotential height fields at five levels are computed, in the attempt to identify the precursor of the AO tropospheric signature; it seems that large-amplitude stratospheric AO anomalies tend to precede large-amplitude tropospheric AO anomalies. However, the mechanism involved in this stratosphere-troposphere coupling has not been clearly identified. In a recent work [15] at least two separate classes of events have been found during which the troposphere is, respectively, isolated from (T events) or linked to (S events) the stratospheric circulation. The T events present an equatorward propagation of tropospheric waves in the midlatitudes, followed by a development of westerly anomalies in the high latitudes. On the other hand, the S events show stronger westerly anomalies at the subtropical stratopause level first; these anomalies propagate poleward and downward, causing a deflection of planetary waves from the polar stratosphere to the equatorial troposphere. The S events are suggested as a possible preconditioning for the strenght of the AO during the late winter, while during the early winter the AO seems to be produced solely by tropospheric processes.

In this paper we wish to give a contribution to the understanding of the stationary wave variability at the midtropospheric and lower stratospheric levels that can be related

TABLE I. – *The explained variance of the first four EOFs for the anomaly fields.*

	EOF1	EOF2	EOF3	EOF4
SLP	22	13	9*	8*
H500	18	13	9	6*
H50H	49	15	10	6

to the NAO fluctuations. As many other studies, it relies upon a Principal Component Analysis (PCA) and a Singular Value Decomposition (SVD) ([16], see also Appendix for a short review of the method) of the anomaly fields of sea level pressure (SLP), geopotential fields at 500 and 50 hPa (H500 and H50H) and 200 hPa zonal wind component (U200).

After a brief discussion on the results of the PCA applied to the anomaly fields (sect. **2**), we will focus on the interannual variability of the eddy fields for the middle troposphere and the lower stratosphere. The variability of the tropospheric and stratospheric eddy components related to the NAO has not been extensively described in other works. In particular following Rossby (see also ref. [17]), we divide the circulation as the mean averaged component and the deviation from it. Then we apply the PCA to the eddy fields (sect. **3**), evaluated on the same data set. In sect. **4** the dynamical link between jets and eddy fields is analyzed. Conclusions are given in sect. **5**.

The main results are the identification of the NAO signature onto the middle tropospheric and lower stratospheric eddy fields. In particular the covariance analysis (SVD) between the eddy fields and the zonal component of the wind field at 200 hPa level (jet core level) seems to carry the signature of the PNA and NAO. At the middle tropospheric level, the eddy PNA mode seems to relate the Pacific and the Atlantic jet when they are zonally elongated, while the eddy NAO mode shows an asyncronous behaviour. In the stratosphere, the PNA and NAO associated with wind modes show a correspondence with wave number two patterns.

2. – Data, methods and preliminary analysis

The data set used in this work is the National Centers for Environmental Prediction-National Center for Atmospheric Research (NCEP-NCAR) reanalysis ([18]), provided by the National Oceanic and Atmospheric Administration (NOAA) Climate Diagnostics Center (CDC). Extended winter (DJFM) geopotential heights (50 hPa and 500 hPa), sea level pressure and zonal wind (200 hPa), for the region from 20 N to the North Pole are used on a regular 2.5×2.5 grid. The data set covers winter months from 1948 to 1999.

The seasonal cycle has been removed by subtracting the calendar monthly means.

TABLE II. – *The correlation coefficient between the principal component time series, associated with the anomaly EOFs, and the NAO index for the period of record 1947-1998.*

	EOF1	EOF2	EOF3	EOF4
SLP	77:83	7:24	42:31	$-25:-22$
H500	59:57	60:68	$-33:-23$	$3:-21$
H50H	37:39	$-7:-19$	17:23	3:5

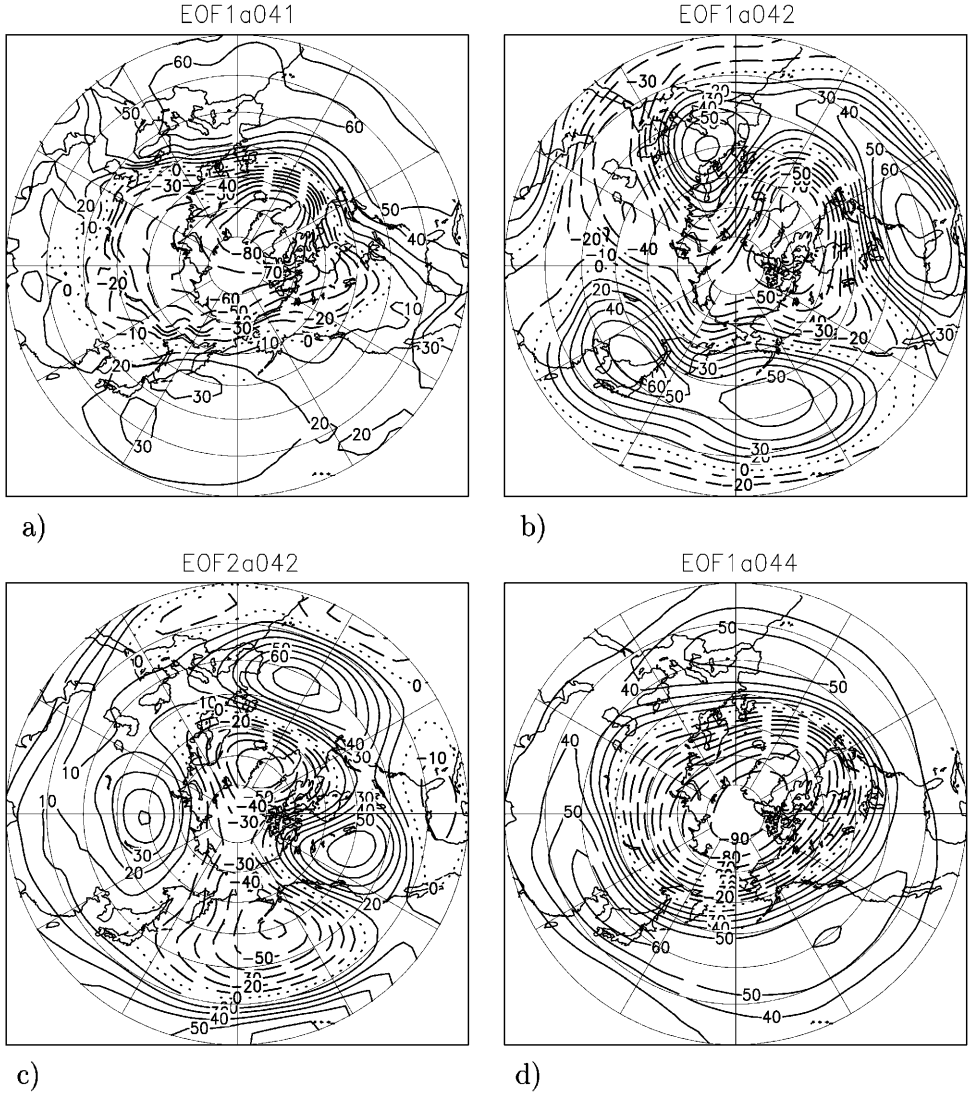

Fig. 1. – Correlation pattern for the extended wintertime (JFMD): a) the first eigenvector of sea level pressure; b) the first eigenvector of the wintertime 500 hPa geopotential height anomalies; c) the second eigenvector of the wintertime 500 hPa geopotential height anomalies; d) the first eigenvector of the wintertime 50 hPa geopotential height anomalies.

The PCA has been applied separately to each field. To ensure that equal areas provide equal weights in the analysis, winter mean data are weighted by the square root of cosine of latitude. For each field, we construct two covariance matrices: one for the anomaly field time series and one for the eddy anomaly field time series.

In fig. 1a we display the first eigenvector of the covariance matrix of the sea level pressure for the extended winter (DJFM). In order to compute the correlation pattern, the empirical orthogonal function is multiplied by the square root of the eigenvalue and

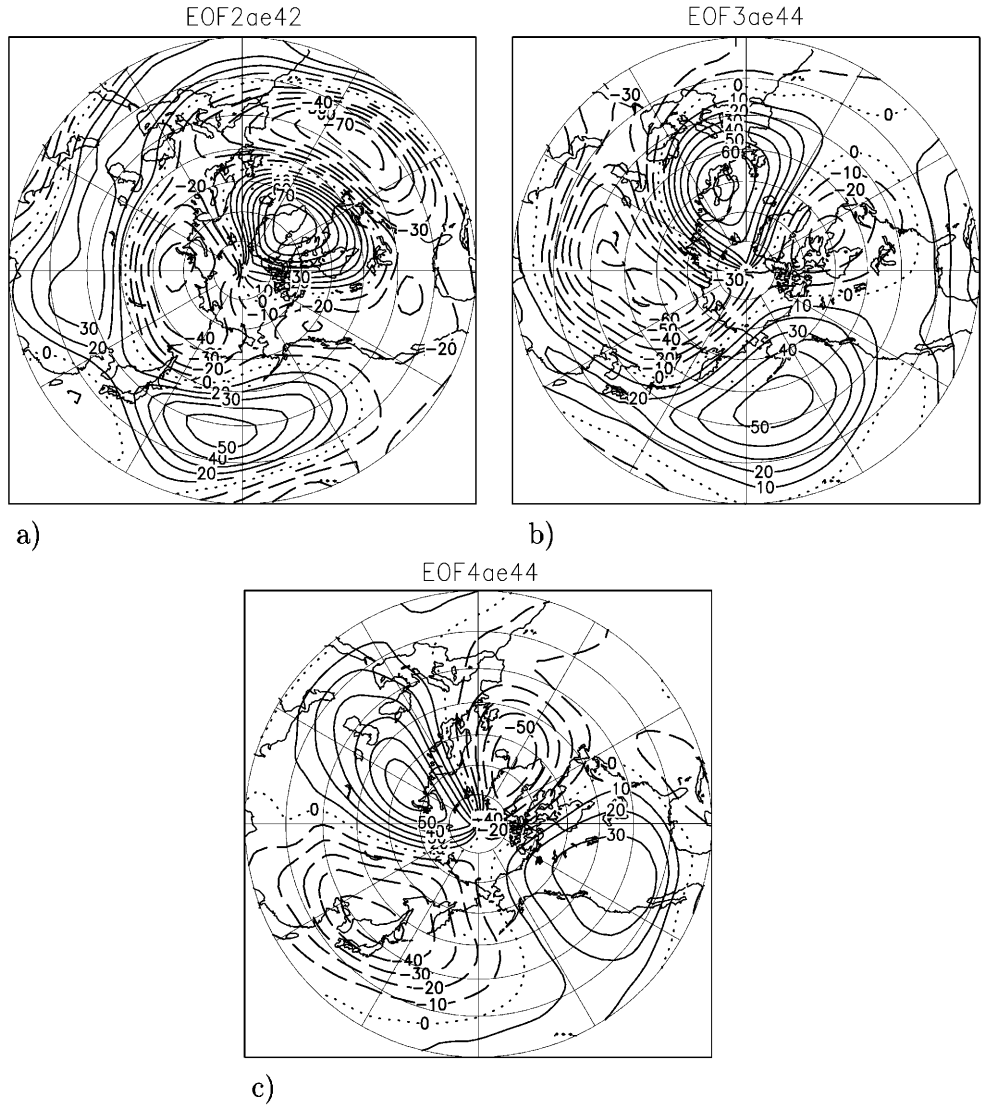

Fig. 2. – Correlation pattern for the extended wintertime (JFMD): a) the second eigenvector of the wintertime 500 hPa geopotential height eddy anomalies; b) the third eigenvector of the wintertime 50 hPa geopotential height eddy anomalies; c) the fourth eigenvector of the wintertime 50 hPa geopotential height eddy anomalies.

normalized by the standard deviation of the field. The pattern is similar to the ones shown in other studies [6, 9], although here the Atlantic center of action appears to have a stronger loading. The SLP loading factor shows a dipole structure with a negative center of action covering the pole and the northern sectors both of Asia and America. The absolute maximum appears to be located over Iceland and Greenland. A strong positive center is also present in the central and southern European region. A weak center of action over the western Pacific is also noticeable. The Northern Hemisphere

pattern resembles the annular mode of ref. [6], but with the Pacific center weaker and westernmost. The PC time series (figure not shown) show a slight negative trend in the first part of the time series and three bursts in the last three decades which are roughly sinchronous to the NAO peaks as observed in ref. [3].

In table I, we report the variance explained by the first four EOFs for SLP, H500 and H50H; following the rule proposed by ref. [19], the asterisk denotes that the eigenvalues of two neighbouring modes cannot be separated from each other due to the sampling error. In this case an asterisk on the third mode means that the third and fourth cannot be separated and so on.

In table II, the correlation coefficients between the principal component time series associated with the aforementioned patterns and the NAO index (see ref. [3]), are reported. The table shows two values, the first for the unfiltered time series, the second for the time series where the intra seasonal variability has been removed (winter time series).

The first mode of the SLP accounts for the 22% of variance (see table I), and it shows good correlation with the NAO index 77% (83%). Good correlation with the NAO index can also be found in the middle troposphere: the first and second mode for H500 show a correlation coefficient of about 60%. The correlation value decreases into the lower stratosphere where the maximum is attained by the first mode (37–39%).

Figures 1b and 1c show the first and second loading for the H500 field, explaining respectively 18% and 13% of the total variance. The pattern of the first loading captures a structure similar to the one identified by ref. [14] and ref. [6]. The main positive centers are located over the central and western Pacific, the Atlantic US coasts and northern Europe, while the negative centers lay over Greenland, the Labrador sea, and eastern Europe. The two positive centers in the Atlantic sector are probably related to the storm track interannual variability. In fact, as discussed in ref. [20] similar centers are detected through a singular value decomposition of the 250 hPa zonal wind and the transient eddies. The second H500 loading (fig. 3) shows what seems to be a combination of PNA anomaly pattern and North Atlantic dipole pattern, with a weak center of action over northern Asia, which can be considered as a third pole of an eventual wave train propagating from the tropical Atlantic. These two patterns, strongly related to the NAO variability, do not show a relevant annular structure.

We consider also the first EOF in the lower stratosphere (H50H field), which shows a low correlation on the interannual time scale (37%). We observe a symmetric mode (fig. 1d) with a center of action displaced slightly off the pole towards Greenland and an annular band over midlatitudes. This picture is quite similar to that shown in ref. [14].

In summary, this analysis seems to indicate that an annular mode is evident only in the lower stratosphere where it weakly correlates with the NAO index. The reverse occurs in the troposphere, where the NAO behaviour strongly correlates with the SLP and H500 loading modes, which however barely show an annular structure.

3. – Zonal-eddy anomaly field analysis

The atmospheric circulation variability can be also represented by considering its zonally symmetric and eddy (or stationary-wave) components [21]. Along this line, the PCA analysis has been extended to the eddy anomaly covariance matrix and to the zonal anomaly covariance matrix. The PCA has been applied to the 500 hPa geopotential height and 50 hPa geopotential height (hereafter refered as EH500, EH50H for the eddy component and ZH500, ZH50H for the zonal component). In table III we show the

TABLE III. – *The explained variance of the first four EOFs for the eddy anomaly and the zonal fields.*

	EOF1	EOF2	EOF3	EOF4
EH500	18	13	10*	9*
EH50H	33	26	14	10
ZH500	58	–	–	–
ZH50H	83	–	–	–

explained variance of the first four EOFs and in table IV the correlation between the PCs and the NAO index. The explained variance of the eddy components decreases slowly with the order of the EOF as in the anomaly analysis, although the decreasing rate is lower. For the zonal fields we present only the first mode, which represents a "zonal-index mode" and takes into account most of the variance (58% and 83% for ZH500 and ZH50H, respectively).

It appears from table IV, that in this case the NAO index is connected to the second loading of the EH500 and to the third and fourth loadings of EH40H. In the case of EH500 field the value of the correlation is high −77% (−84%), while the third and fourth EH50H loadings show lower values, 44% (52%) and 41% (41%), respectively. In the case of the EH50H field the temporal smoothing produces a higher coefficient value for the third loading.

The correlation coefficients of the loadings of the zonal index show the following values: −62% (−64%) for the ZH500, and −36% (−39%) for the ZH50H. The correlation coefficient values of the other zonal loadings (not shown) are significantly lower.

The EH500 EOF2 pattern (fig. 2a) shows two dipolar structures over the Euro-Atlantic and the Asian sectors, which can be part of the wave train observed also in fig. 1c, and a positive center of action over the western Pacific. Finally, the patterns of fig. 2b and 2c show the center of actions of the 50 hPa geopotential height variability. The most relevant feature is a dominating zonal wave number two in both the EOFs. The third EOF shows positive centers over Scandinavia and Alaska, and a strong negative pole over eastern Asia. The fourth EOF shows positive centers over western US coast and central Asia, and negative centers over Greenland and Iceland, and over Japan.

The wave patterns of variability appear to be dynamically linked with the jet fluctuation. For illustrative purpose, the positive (negative) composites of NCEP 200 hPa zonal wind, for low (high) PC index, have been computed. In fig. 3a (3b) the difference between the composites and zonal wind climatology corresponding to positive (negative) phase of the EH500 PC2 time series, is shown. The positive phase shows a strengthening and a

TABLE IV. – *The correlation coefficient between the principal component time series, associated with the EOFs of table III, and the NAO index for the period of record 1947-1998.*

	EOF1	EOF2	EOF3	EOF4
EH500	12:6	−77 : −84	−18 : 7	8:26
EH50H	2:15	−2 : 1	44:52	41:41
ZH500	−62 : −64	–	–	–
ZH50H	−36 : −39	–	–	–

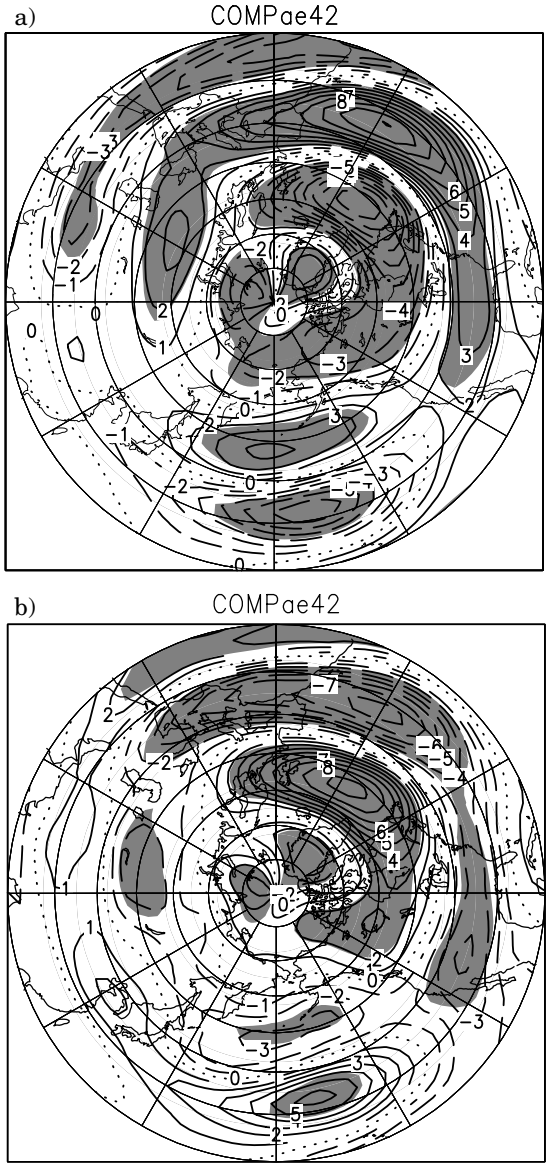

Fig. 3. – U200 composites patterns corresponding to a) +1 standard deviation b) −1 standard deviation of the score time series of the EH500 second EOF. The climatology has been subtracted. Statistically significant values are shaded.

zonal elongation of the Atlantic jet, a weakening of the Arabian jet magnitude, a weak signature over the central Pacific can also be observed, indicating a zonal contraction both of the jet core and of the jet exit. In the negative phase, we observe the signature of the strong northward shift of the Atlantic jet exit. Similar features are observed in the composites for the EH50H PC4 (figure not shown). Figure 4 is the analog of fig. 3 for the EH50H PC3. The positive phase indicates a northward shift of the Atlantic jet

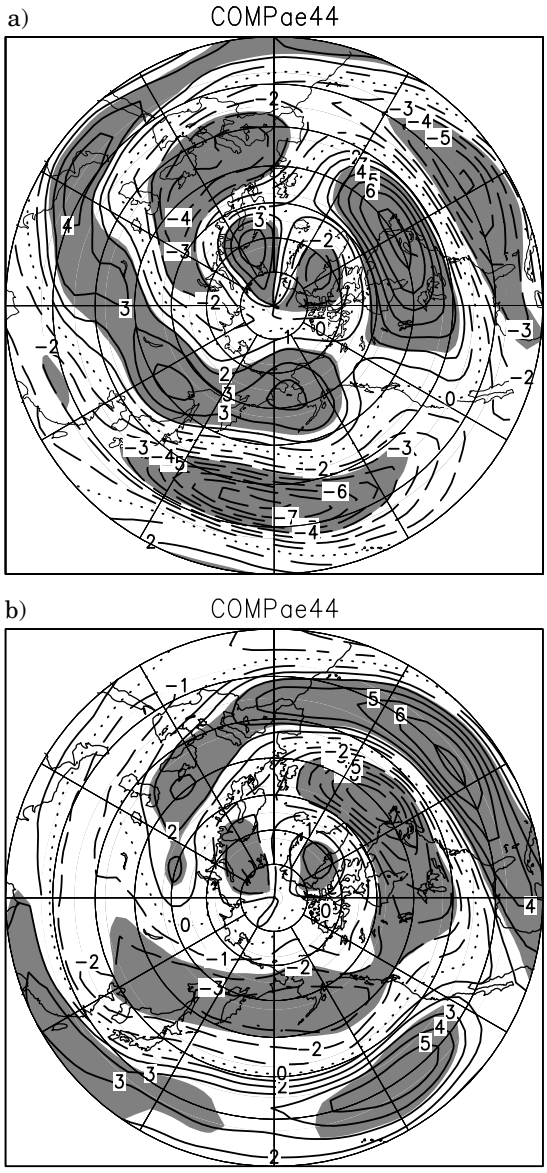

Fig. 4. – U200 composites patterns corresponding to a) +1 standard deviation b) −1 standard deviation of the score time series of the EH50H third EOF. The climatology has been subtracted. Statistically significant values are shaded.

core over the North American coast, a shortening of the Pacific jet in the zonal direction and a strengthening of the Arabian jet. The negative phase shows a southward shift of the Atlantic jet core, and a greater zonal extension of the Pacific jet. It is interesting to note that, for the negative phase of EH50H PC3, a southward shift of the Atlantic jet and its zonal elongation seems accompained by strengthening and elongating eastward of the Pacific jet. On the contrary in the positive composite of EH500 PC2, the strong

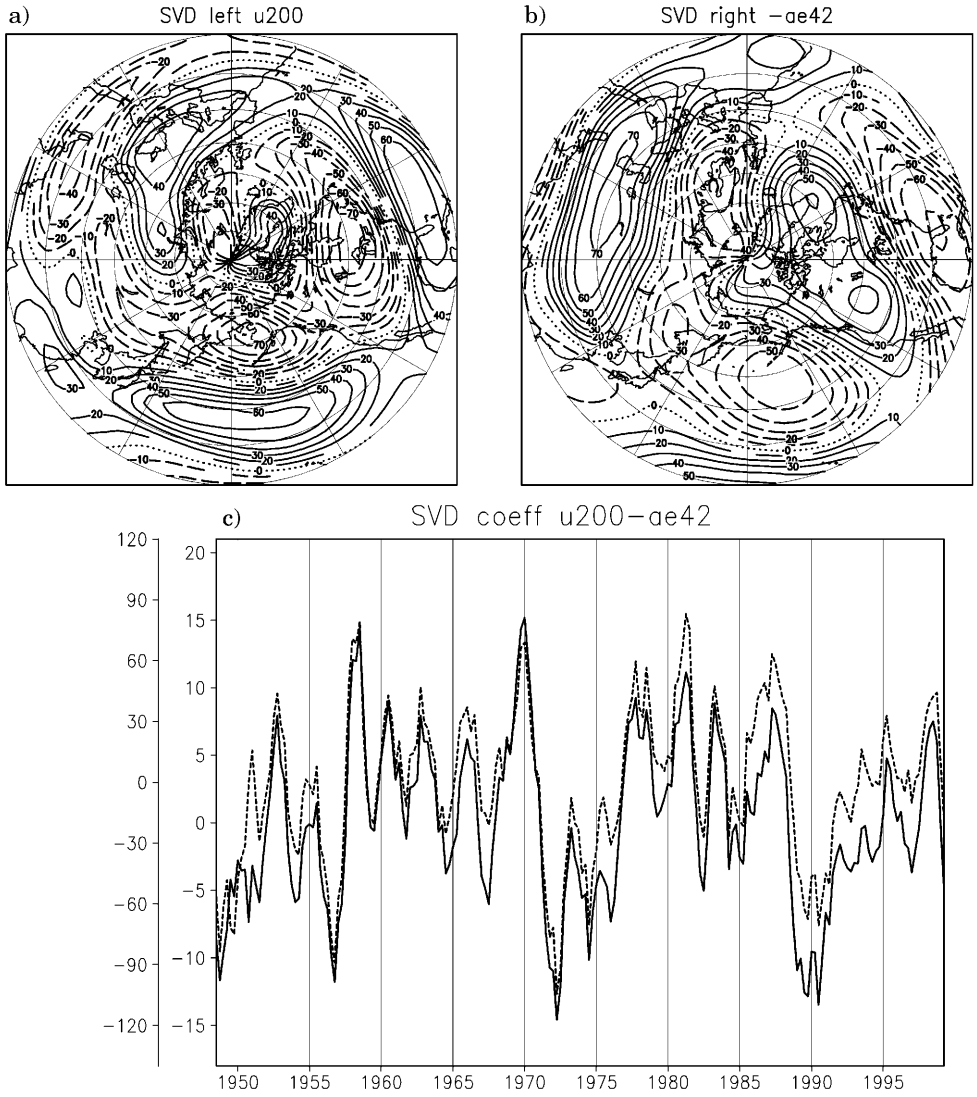

Fig. 5. – SVD left and right first vectors (a-b) for U200 and EH500 fields. c) Score time series.

zonal elongation of the Atlantic jet seems to be related to a weakening and contraction of the Pacific counterpart. The EH500 variability seems to be more related to the jet exit fluctuations on the Atlantic sector, while the EH50H pattern has a more hemispheric link and a strong relationship with the Atlantic jet core.

In summary, the comparison between the analysis performed using the anomaly field and the eddy anomaly field suggests that the NAO variability can be better identified in the eddy anomaly fields, by comparing the correlation coefficients between the loading scores and the NAO index.

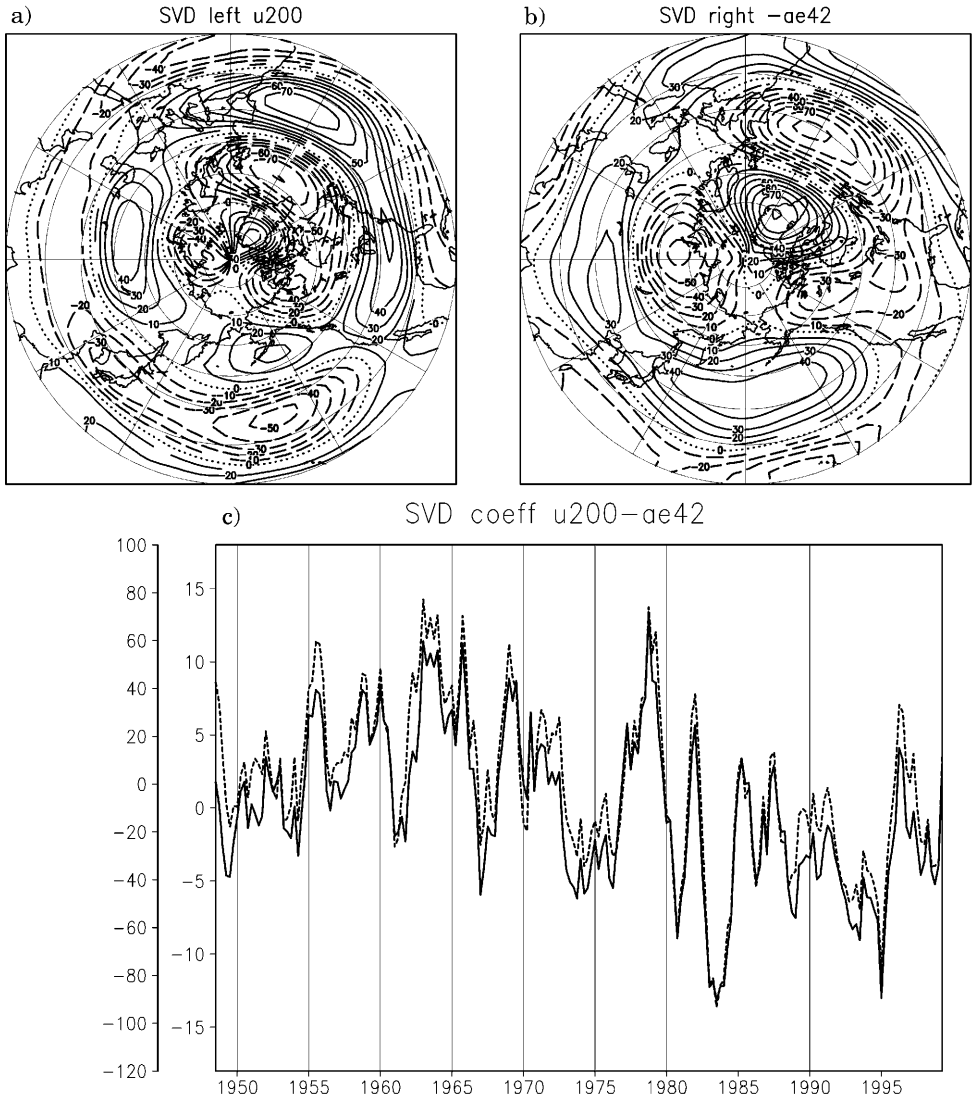

Fig. 6. – SVD left and right second vectors (a-b) for U200 and EH500 fields. c) Score time series.

TABLE V. – *Square Covariance Fraction for the first four SVD vectors.*

	SVD1	SVD2	SVD3	SVD4
U200-EH500	47	21	15	9
U200-EH50H	33	26	13	7

TABLE VI. – *The correlation coefficient between the SVD scores time series, associated with the SVD of table V, and the NAO index for the period of record 1947-1998.*

	AK1	BK1	AK2	BK2
U200-EH500	−53 : −45	−43 : −35	−72 : −81	−65 : −73
U200-EH50H	−55 : −48	−26 : −21	−77 : −84	−43 : −57

4. – Jets-eddy circulation covariability

In the previous section we have separately identified the NAO modes of the eddy component of the 500 hPa and 50 hPa geopotential heights. Now we explore the covariability of the NH jets and the eddy components. A SVD decomposition is applied to isolate significant coupled modes in the time series of the two fields. The zonal wind component at the jet core level (200 hPa) is covaried with the middle tropospheric eddy component and with the lower stratospheric eddy component.

Figure 5 shows the left and right SVD vectors of the first mode for U200-EH500 and the time series of the corresponding expansion coefficients. The squared covariance fraction values (SCF) are shown in table V, in this case the value is 33%. The left vector is quite similar to the composite patterns of fig. 4, with the main centers located over central Pacific and over the US west coast. The Pacific center represents the zonal elongation and reduction of the Pacific jet, while the US coast dipole describes the meridional shift of the Atlantic jet core. The right vector shows a PNA wave train and a strong center of action over central Asia.

The second SVD vector (fig. 6, SCF 26%) mostly projects on the Euro-Atlantic sector. The left vector shows the dipole over the eastern Atlantic, representing the fluctuation of the jet exit, and a negative center of action over the Pacific. The right vector shows a wave train starting from the eastern Atlantic, as in second loading of EH500 (fig. 2a).

Figure 7 shows the left and right SVD vectors of the first mode for U200-EH50H (SCF 47%) and the time series of the corresponding expansion coefficients. The left vector shows the same centers of action of the U200-EH500 left pattern, with lower correlation values. On the other hand the wave number two pattern, observed in the EOF3 of EH50H, is clearly represented by the right vector.

The second SVD left vector (fig. 8, SCF 21%) projects mostly on the Euro-Atlantic sector, as for the second U200-EH500 left vector (fig. 6). The right vector shows a wave number two pattern which strongly resembles the EOF4 of EH50H (fig. 2c).

The correlation between the SVD scores and the NAO index (table VI) shows that the second SVD modes, both for 50 and 500 hPa geopotential height, are those most linked to the NAO variability, as has been suggested by the pattern analysis.

5. – Conclusions

In summary, the analysis performed suggests that the eddy patterns of variability allow a better identification of the modes connected to the NAO in the middle troposphere and in the lower stratosphere, compared to the anomaly fields and the zonal index.

At the midtroposphere level the eddy variability analysis shows an eastern Atlantic dipole and a corresponding Asian dipole that together can form a wave train pattern, higly correlated with the NAO mode, the analysis of the lower stratosphere detects two

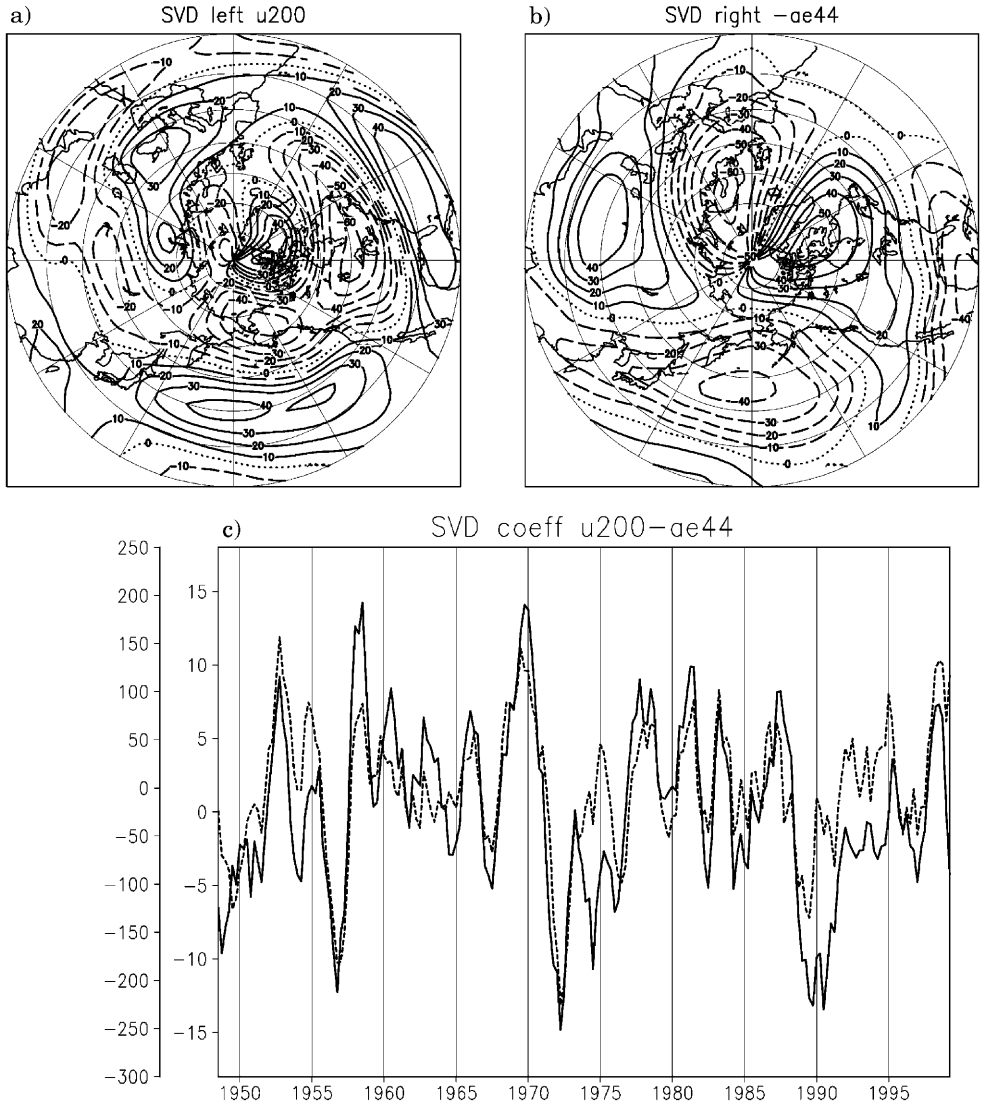

Fig. 7. – SVD left and right first vectors (a-b) for U200 and EH50H fields. c) Score time series.

modes which have a weak NAO correlation, both patterns showing a wave number two.

The covariance analysis and the comparison with the eddy EOFs have revealed the following points:

– the U200 pattern that explains most of the covariance with EH500 and EH50H fields is a PNA pattern; while the second U200 pattern can be defined as a NAO mode;

– the U200 PNA mode syncronizes the two jets zonal elongations;

– the U200 PNA mode shows a strong link with the lower stratosphere represented

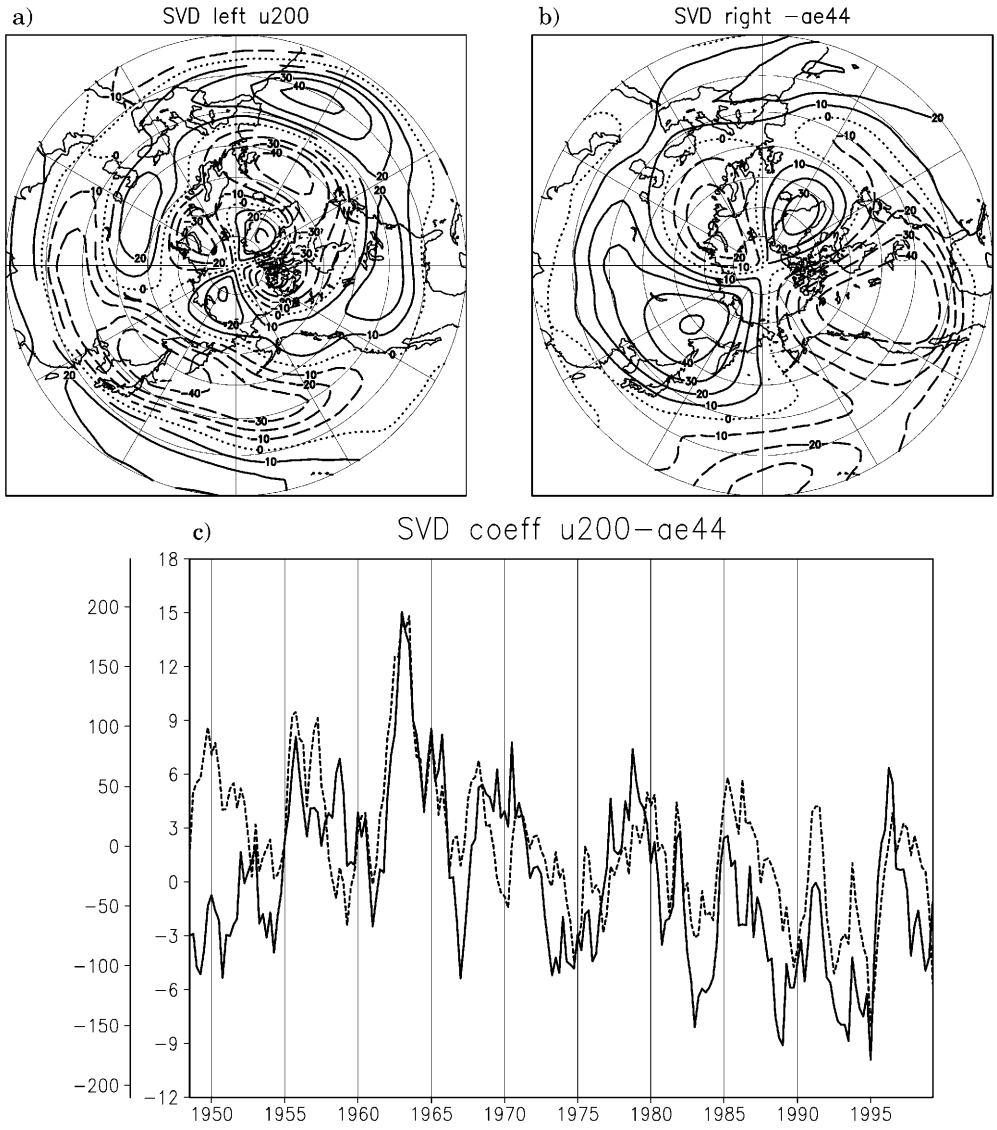

Fig. 8. – SVD left and right second vectors (a-b) for U200 and EH50H fields. c) Score time series.

by a wave number two pattern;

– the U200 NAO pattern does not show any symmetries between Pacific and Atlantic.

The eddy fields have been covaried with the zonal component of the wind field at 200 hPa level. This level represents the jet core level. The jets variability is dynamically linked to the tropospheric wave fluctuations and their propagation up to the stratosphere. The first mode of the SVD analysis between U200 and both EH500 and EH50H represents a PNA mode. When the Pacific jet exit is westward stretched, the Atlantic jet

core is shifted southward and zonally elongated, on the other hand, when the Pacific jet exit is confined back to the date line, the Atlantic jet core is northernmost. The former case shows a tendency to syncronize the zonal elongation of the two jets. The midtroposphere eddy SVD pattern shows a PNA wave train and an eastern-Atlantic western-Asia wave train. The corresponding lower-stratosphere SVD pattern has a wave number two structure as observed into the third EOF of the 50 hPa geopotential height eddies. The connection between the midtropospheric and the lower-stratosphere geopotential height has been highlighted by ref. [13] using the SVD analysis. They found (fig. 8 of their paper) two tropospheric wave trains as in the right pattern of fig. 10, and a stratospheric wave number two pattern similar to the right vector of fig. 12. In the former case their Atlantic-Asian wave train is slightly estward shifted, while in the later case the Pacific center of action is quite different.

The second mode of the SVD analysis shows a western Atlantic dipole and a Pacific center of action. The Atlantic dipole represents the meridional fluctuation of the Atlantic jet exit, strongly related to the NAO variability. In this case the zonal elongation of the Atlantic jet is in counter phase with the zonal reduction of the Pacific jet. The midtropospheric geopotential pattern shows a pattern similar to the eddy NAO mode in the EOF analysis, while the lower stratospheric pattern is a wave number two as in the fourth EH50H EOF.

The main conclusion concerns the relevance of the stationary waves on the NAO; the NAO modes are identified more clearly using the covariance matrix of the eddy anomaly fields. The stratospheric signature of the PNA and NAO U200 modes has been documented in this work. Two wave number two patterns arise from the variance and covariance analysis. These two patterns explain 24% of the total variance, in the PCA analysis, with respect to the 59% of the first two modes (wave number one modes), but they are the principal modes linked to the tropospheric jets fluctuations. The PNA mode sincronizes the Pacific and the Atlantic jets when they zonally elongate. On the other hand, the NAO mode shows an asynocronous behaviour between Atlantic and Pacific sector.

The results presented in this paper seem to confirm the NAO-PNA perspective investigated also by ref. [10]. The analysis of the eddy fields variability into the troposphere and lower stratophere shows distinct modes related to the NAO pattern and to the PNA pattern, both in the middle troposphere and in the lower stratosphere.

It remains to understand the connection between the zonal-mean component and the eddies, in particular if the NAO vertical mode is forced by the zonal-mean component (as suggested by ref. [22]) or it is directly forced by an external forcing (such as SST or stratosphere forcing).

* * *

The authors would like to thank Dr. R. Iacono for his helpful comments, and Dr. P. Ciolli for the previous work in preparing part of the data set used in this paper.

Appendix A.

The singular value decomposition

The singular value decomposition (SVD) identifies pairs of spatial patterns that explain as much as possible the mean-squared temporal covariance between the two fields

considered. The SVD lies on the fact that any general m*by*n real matrix A can be decomposed uniquely as follows:

$$A = P\Sigma Q^T \,, \tag{A.1}$$

where $P(m \times m)$ and $Q(n \times n)$ matrices are both orthogonal, and $\Sigma = \mathrm{diag}\,(\sigma_1, ..., \sigma_r)$, with $r = \min(m, n)$ and $\sigma_1 \geqslant \sigma_2 ... \geqslant \sigma_r$. The σ_i are called singular values, and the first r columns of Q the right singular vectors and the first r columns of P the left singular vectors. The singular values and the singular vectors satisfy

$$Aq_i = \sigma_i p_i \text{ and } A^T p_i = \sigma_i q_i \,, \tag{A.2}$$

where p_i and q_i are the i-th columns of P and Q, respectively.

In geophysical application of the SVD we consider two data fields: $s(x,t)$ with m spatial points and T times and $z(x,t)$ with n spatial points and T times. These two fields are organized in two matrices, S has m rows by T columns and $Z\,n$ rows by T columns. Both time series are supposed to have zero mean. Then the cross-covariance matrix $C = S\,Z^T$ is decomposed as in (1). The first singular value can be written as follows:

$$\sigma_1 = {p_1}^T C q_1 = {p_1}^T S Z^T q_1 \,, \tag{A.3}$$

where ${p_1}^T S$ and ${q_1}^T Z$ are the projection of the data time series onto the corresponding singular vectors. These projections produce two time series of expansion coefficients which can be defined as score vectors a_i and b_i with dimension T. The previous formula becomes

$$\sigma_1 = a_1 {b_1}^T \,. \tag{A.4}$$

Then the choice of the pairs of singular vectors (p and q) maximizes the covariance between the corresponding expansion coefficients.

The total squared covariance explained by a pair of singular vectors is ${\sigma_k}^2$, so it is possible to define the percentage of the covariance explained by a pair of vectors (Squared Covariance Fraction):

$$SCF_k = \frac{{\sigma_k}^2}{\sum_{l=1}^{r} {\sigma_k}^2} \,. \tag{A.5}$$

REFERENCES

[1] Wallace J. M. and Gutzler D. S., *Mon. Weather Rev.*, **109** (1981) 784.
[2] vanLoon H. and Rogers J., *Mon. Weather Rev.*, **106** (1978) 296.
[3] Hurrell J. W., *Science*, **269** (1995) 676.
[4] Hurrell J. W. and van Loon H., *Climate Change*, **36** (1997) 301.
[5] Wallace J. M., *Q. J. R. Meteorol. Soc.*, **126** (2000) 791.
[6] Thompson D. W. J. and Wallace J. M., *Geophys. Res. Lett.*, **25** (1998) 1297.
[7] Thompson D. W. J. and Wallace J. M., *J. Climate*, **13** (2000) 1000.
[8] Thompson D. W. J. and Wallace J. M., *J. Climate*, **13** (2000) 1018.
[9] Deser C., *Geophys. Res. Lett.*, **27** (1999) 779.
[10] Ambaum M. H. P., Hoskins G. J. and Stephenson D. B., *J. Climate*, **14** (2001) 3495.
[11] Baldwin M. P., Cheng X. and Dunkerton T. J., *Geophys. Res. Lett.*, **21** (1994) 1141.

[12] Perlwitz J. and Graf H. F., *J. Climate*, **8** (1995) 2281.
[13] Perlwitz J. and Graf H. F., *Theoretical and Applied Climatology*, **69** (2001) 149.
[14] Baldwin M. P. and Dunkerton T. J., *J. Geophys. Res.*, **104** (1999) 30937.
[15] Kodera K. and Kuroda Y., *Geophys. Res. Lett.*, **27** (2000) 3349.
[16] Bretherton C. S., Smith C. and Wallace J. M., *J. Climate*, **5** (1992) 541.
[17] Molteni F., Sutera A. and Tronci N., *J. Atmos. Sci.*, **45** (1988) 3063.
[18] Kalnay E. and Coauthors, *Bull. Am. Meteorol. Soc.*, **77** (1996) 437
[19] North G. R., Bell T. L., Cahalan R. F. and Moeng F. J., *Mon. Weather Rev.*, **110** (1972) 699.
[20] Carillo A., Ruti P. M. and Navarra A., *Climate Dynamics*, **16** (2000) 219.
[21] Rossby C. G., *J. Mar. Res.*, **3** (1939) 38.
[22] DeWeaver E. and Nigam S., *J. Climate*, **13** (2000) 3893.